Correlation of atmospheric parameters measured by MAGIC optical LIDAR and CTA FRAM

Kolarek, Marta

UNIVERSITY OF RIJEKA

FACULTY OF PHYSICS

Marta Kolarek

CORRELATION OF ATMOSPHERIC PARAMETERS MEASURED BY MAGIC OPTICAL LIDAR AND CTA FRAM

Master thesis

Master’s degree in physics

Astrophysics and physics of elementary particles

Rijeka, 2023.

UNIVERSITY OF RIJEKA

FACULTY OF PHYSICS

CORRELATION OF ATMOSPHERIC PARAMETERS MEASURED BY MAGIC OPTICAL LIDAR AND CTA FRAM

Master thesis

Master's degree in physics

Astrophysics and physics of elementary particles

Mentor: prof. dr. sc. Dijana Dominis Prester

Student: Marta Kolarek

Rijeka, 2023.

TABLE OF CONTENTS

ABSTRACT

The Earth's atmospheric realm is a dynamic force that exerts a profound impact on the planet's climate and natural operations. Astronomical research faces a significant challenge in precisely measuring atmospheric parameters, which directly impact the quality and reliability of observational data. In response, cutting-edge technologies have emerged, including Light Detection and Ranging (LIDAR) and the Foto Robotic Atmosphere Monitor (FRAM) telescope. This research attempts to elucidate the correlation between two vital technologies: the MAGIC LIDAR and CTA FRAM. Specifically, the investigation delves into the relationship between Vertical Aerosol Optical Depth (VAOD), a key atmospheric parameter signifying aerosol content, as measured by these instruments. By analyzing the interplay between VAOD measurements from MAGIC LIDAR and CTA FRAM, this study seeks to refine our comprehension of atmospheric dynamics and enhance the accuracy of both atmospheric science and astronomical observations. The insights gained from this correlation hold the potential to advance our understanding of the Earth's atmosphere and its intricate connections to celestial phenomena.

Key words: MAGIC, CTA, Cherenkov telescopes, LIDAR, FRAM, atmospheric parameters, correlation, VAOD

SAŽETAK

Zemljina atmosfera predstavlja dinamičan sustav koji duboko utječe na klimu planeta i prirodne procese. Astronomska istraživanja suočavaju se s izazovom preciznog mjerenja atmosferskih parametara, što izravno utječe na kvalitetu i pouzdanost promatračkih podataka. Kao odgovor na to, razvijene su napredne tehnologije, uključujući *Light Detection and Ranging* (LIDAR) i teleskop *Foto Robotic Atmosphere Monitor* (FRAM). Ovo istraživanje pokušava pokazati povezanost između dvije ključne tehnologije: MAGIC LIDAR i CTA FRAM. Konkretno, istraživanje istražuje odnos između vertikalne optičke dubine aerosola (VAOD), ključnog atmosferskog parametra koji označava prisutnost aerosola, kako ga mjere ovi instrumenti. Analizom međuodnosa mjerenja VAOD-a s MAGIC LIDAR-om i CTA FRAM-om, ovo istraživanje nastoji poboljšati naše razumijevanje dinamike atmosfere i povećati preciznost kako u znanosti o atmosferi tako i u astronomskim promatranjima. Rezultati dobiveni iz ove korelacije imaju potencijal za napredak u razumijevanju Zemljine atmosfere i njezinih složenih veza s nebeskim pojavama.

Ključne riječi: MAGIC, CTA, Čerenkovljevi teleskopi, LIDAR, FRAM, atmosferski parametri, korelacija, VAOD

1. INTRODUCTION

The Earth's atmosphere plays a fundamental role in shaping our planet's climate and influencing various natural processes. Understanding the intricate dynamics of atmospheric parameters is crucial for a wide range of scientific disciplines, including meteorology, climatology and astrophysics. Among the various challenges faced by astronomers, one of the most crucial is the accurate measurement and monitoring of atmospheric parameters, as these can significantly impact the quality and precision of astronomical data. Advanced technologies and instruments have been developed to observe and measure atmospheric components accurately.

Among the radical technologies that have transformed atmospheric research, Light Detection and Ranging (LIDAR) stands out as a remarkable innovation. By directing laser pulses, LIDAR systems have the ability to remotely detect and quantify a wide range of atmospheric properties, offering researchers invaluable data for in-depth analysis.

The advent of LIDAR technology has initiated in a new era in atmospheric studies, providing scientists with a non-intrusive and accurate means to investigate our planet's complex air composition. MAGIC LIDAR, with its multiwavelength capabilities, has the potential to shed light on previously elusive aspects of the atmosphere, allowing researchers to deepen their understanding of atmospheric processes and their implications for the broader environment.

On another hand, Foto Robotic Atmosphere Monitor (FRAM) telescope, which is used to meticulously track the Earth's atmosphere and its optical characteristics represents a significant development in modern astronomy.

The FRAM telescope is essential in improving the accuracy and reliability of astronomical observations because it focuses on the dynamic behavior of aerosols, which are tiny suspended particles that include dust, pollution, and water droplets. Its importance comes in its capacity to provide crucial information that clarifies the impact of atmospheric factors on high-energy astrophysical events, strengthening the foundation of our knowledge of the cosmos.

This research attempts to explore the relationship between various atmospheric properties, such as aerosol content, temperature profiles, and water vapor distribution, as measured by the MAGIC LIDAR and CTA FRAM. To better comprehend how the environment affects the formation of cosmic ray showers and Cherenkov radiation, which we monitor with Cherenkov telescopes in astrophysics, finding a correlation is essential. This association study is crucial because it can offer

important information about how the atmosphere affects these events. We may better understand these intricate processes by identifying the links between atmospheric factors and cosmic air showers, as well as their connection to Cherenkov radiation. In the end, this study can improve our Cherenkov telescope data and help us understand how the atmosphere shapes cosmic events.

Moreover, investigating the correlation between MAGIC LIDAR and CTA FRAM measurements will not only improve our comprehension of atmospheric dynamics but also refine the calibration techniques used in astrophysical experiments.

2. ATMOSPHERIC PARAMETERS

The Earth's atmosphere is a complex and multidimensional system that surrounds our planet and supports life as we know it while also regulating its climate. This atmospheric barrier, which is made up of layers with different compositions and characteristics, interacts with solar radiation, cosmic rays, and the Earth's surface to influence weather patterns, climate dynamics, and the delicate balance of greenhouse gases. The greenhouse effect, which is the term used to describe the blockage of incoming radiation by the atmosphere, prevents the Earth's surface from being as cold as it would be in the absence of an atmosphere. Diatomic nitrogen (N_2), which makes up about 78 % of the atmosphere of the Earth, predominates, followed by oxygen (O_2), which makes up about 21 %. Compared to neon, helium (He), krypton (Kr), and xenon (Xe), argon (Ar) is present in significantly higher amounts. Approximately 0.25 % of the mass of the atmosphere is made up of the highly variable gas known as water vapor. Molecules with carbon, nitrogen, and sulfur atoms that were formerly absorbed into the cells of living beings are among the trace gaseous components of the atmosphere. These gases are released into the atmosphere when fossil fuels and plant material are burned, when plants produce emissions, and when plants and animals decompose. Even though aerosols and cloud droplets only make up just a small percentage of the atmosphere's mass, they play an important role in the hydrologic cycle's atmospheric branch by mediating the condensation of water vapor, taking part in significant chemical reactions, acting as the sites of these reactions, and producing a range of optical effects, including electrical charge separation. [18]

In atmospheric physics, many atmospheric parameters are used to describe various aspects of atmospheric dynamics and physics, and the most common ones are temperature, pressure, air density, humidity, wind speed and direction, visibility, cloud cover, vertical aerosol optical depth (VAOD), and others.

2.1. Pressure and air density

The first two key atmospheric parameters are air pressure and density. The force that an area of the Earth's surface is subjected to due to the weight of air molecules is known as atmospheric pressure. As air molecules travel randomly, clash with one another, and surface, pressure is applied in all directions. The pressure felt at a specific spot is the result of these molecular collisions adding together. The air pressure changes with altitude, typically dropping as one

rises higher due to the decrease in the number of air molecules in the atmosphere. Weather patterns and atmospheric circulation are significantly influenced by atmospheric pressure. The movement of air masses is influenced by variations in regional pressure, which results in the formation of high-pressure systems and low-pressure systems. As the air descends and stifles cloud formation, high-pressure systems are linked to clear skies and steady weather. As air rises and cools, causing condensation and cloud production, low-pressure systems are characterized by unpredictably bad weather, cloud formation, and the potential for precipitation. [18]

How closely the air molecules are packed together inside a specific volume of space is determined by the atmospheric density. Because there are fewer air molecules and less pressure as one ascends higher in the atmosphere, the density often drops. At sea level, the air has a density of 1.25 kg/m^3. Similar to how pressure drops with height, so does density. The equivalent horizontal and time variations are substantially smaller than these vertical differences in pressure and density. In order to illustrate the averaged horizontal and temporal structure of the atmosphere as a function of height alone, as shown in *Fig. 1*, it is useful to set up a standard atmosphere. The fact that the observed vertical profiles of pressure and density on these semilog plots closely resemble straight lines suggests that pressure and density depend roughly exponentially on height. [18]

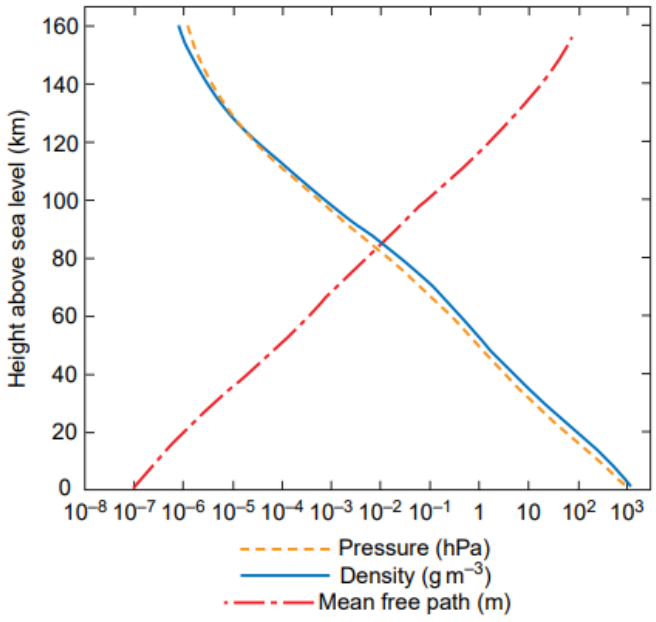

Figure 1. Vertical profiles of pressure and density [16]

2.2. Temperature

The temperature of the atmosphere is another important factor. Numerous natural phenomena are supported by temperature, which is a fundamental physical attribute. The average kinetic energy of the individual particles that make up a substance is measured by temperature, which has its roots in the kinetic theory of matter. This theory states that all matter is made up of atoms and molecules that are constantly and randomly moving. These particles have kinetic energy, which is a measure of how fast they are moving. When the temperature is higher, the particles move more quickly and fiercely, while when the temperature is lower, their motion becomes more sluggish. Specifically, atmospheric temperature is a measurement of the typical kinetic energy that air molecules in a particular area of the atmosphere possess. The gas particles move randomly as a result of the Sun and other radiant energy sources' absorption and emission, creating this kinetic energy.

The vertical distribution of temperature for typical conditions in the Earth's atmosphere provides a basis for dividing the atmosphere into layers, and they are as follows: troposphere, stratosphere, mesosphere and thermosphere. Each layer has its own characteristics, which we will briefly describe. We live in the troposphere, which starts at the surface and rises to an average altitude of 10 kilometers. This layer provides the oxygen required for respiration and sustaining life as we know it. The air pressure and temperature drop as we move upward through this layer, requiring adaptations for life at greater altitudes. However, within the troposphere, there are a few thin layers where the temperature rises with height, known as temperature inversions, and these hinder vertical mixing significantly.

The stratosphere, which rises to a height of about 50 kilometers, is found above the troposphere. The ozone (O_3) layer, which is located between 10 and 50 kilometers above the Earth's surface, is a distinguishing characteristic of this layer. The stratospheric ozone molecules are essential for absorbing and reducing the sun's damaging ultraviolet (UV) radiation. By limiting excessive UV exposure, this protection protects Earth's life from negative impacts. Just as it occurs within the much thinner temperature inversions that occasionally form within the troposphere, the increase in temperature with height greatly inhibits vertical mixing. As we ascend, we reach the mesosphere, which is about 85 kilometers or so above the Earth's surface, and in this region, the temperature drops as we ascend, resulting in extremely low temperatures. The thermosphere comes after the mesosphere. The breakdown of diatomic nitrogen and oxygen molecules, the loss of

electrons from atoms, and the absorption of solar radiation are all responsible for the increase in temperature with height within the thermosphere. These actions are known as photoionization and photodissociation. The described atmospheric layers and their temperature gradients are visually illustrated in *Figure 2*. [18]

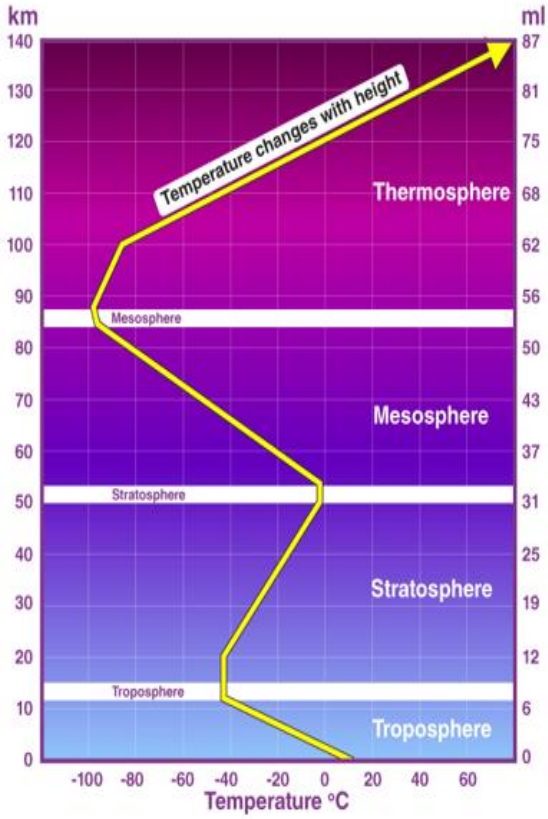

Figure 2. Temperature gradient diagram of different layers of atmosphere [3]

2.3. Humidity

The atmosphere contains an indispensable element known as humidity, which refers to the amount of water vapor present in the air. Typically stated as a percentage, it indicates the proportion of water vapor relative to the air's maximum capacity at a specific temperature. This humidity factor significantly impacts cloud formation and precipitation development.

As warm and moist air rises and cools, it reaches its dew point, resulting in the condensation of water vapor into minute water droplets, eventually giving rise to clouds and various forms of precipitation, such as rain or snow. [18] Astronomy relies heavily on understanding humidity's effects, particularly when it comes to "atmospheric seeing,"

which influences celestial observations. The quality of astronomical images greatly depends on favourable viewing conditions. However, high humidity levels pose challenges to ground-based telescopes, especially those situated in humid regions.

Another issue arrives from the absorption of certain light wavelengths by water vapor, particularly in the infrared region of the electromagnetic spectrum. This absorption can restrain astronomers from observing infrared-emitting objects or events effectively.

To address these challenges, astronomers frequently install telescopes in dry, high-altitude environments to minimize the impact of water vapor on their views.

2.4. Wind speed and direction

The velocity at which air is traveling through a particular place horizontally is referred to as the wind speed. From one place to another, wind speed can differ greatly and change quickly over brief periods of time. It is affected by a number of variables, including as the Coriolis effect (result of the Earth's rotation causing a change in the direction of moving), frictional effects close to the Earth's surface, local topography, and the pressure gradient force which results from differences in air pressure between two locations. Weather and climate are significantly influenced by wind speed. Increased evaporation from water bodies caused by high wind speeds can modify humidity levels and have an impact on cloud and precipitation production. [18] Clouds are very important in astronomy because their presence makes it difficult for scientists to observe and study objects they are interested in using telescopes. Therefore, understanding all the atmospheric parameters that influence the formation and movement of clouds is crucial in astronomy.

2.5. Visibility

The atmospheric visibility is the next parameter. Because it directly influences the clarity and caliber of observations taken from the surface of the Earth or from ground-based observatories, it is essential to astronomy. Astronomers need to be able to observe far-off celestial objects with excellent clarity and resolution in order to carry out reliable study and make significant discoveries. The horizontal distance at which a stationary observer can make out and distinguish recognizable things on the Earth's surface or in the atmosphere is

known as visibility. Unfortunately, factors like fog, which is a low-lying cloud formed by the condensation of water vapor near the Earth's surface, can significantly reduce visibility. Similarly, aerosols such as dust, smoke, haze, and pollution particles, along with water droplets in the air, can scatter and absorb light, further blocking visibility. Astronomers are in a difficult situation because of the air conditions present close to the surface of the Earth. Their observations are faced with significant difficulties in these lower locations due to light pollution, turbulent air, and atmospheric distortions. To overcome these limitations, astronomical observatories purposefully choose isolated areas and higher elevations where the atmosphere is clear, to get beyond these obstacles. [9]

In such protected areas, the impact of light pollution is minimized, and atmospheric stability is at its best, resulting in improved visibility and clear observations, free from the distortions and scattering that plague observatories at lower elevations.

An excellent example of this strategy is the observatory Roque de los Muchachos, which houses the MAGIC LIDAR and CTA FRAM telescopes at an altitude of 2396 meters. By selecting elevated sites like this, astronomers can escape the adverse effects of light pollution and obtain clearer views.

Furthermore, visibility is closely related to another important atmospheric parameter: the presence of clouds, which will be explained in the following chapter.

To achieve the best possible conditions for studying the universe, astronomers continually seek locations with optimal atmospheric clarity and minimal interference from clouds and other atmospheric factors.

2.6. Cloud cover

Typically, the percentage of the sky that is covered by clouds is referred to as cloud cover. A cloud cover of 100 % indicates that the entire sky is obscured by clouds, leaving no visible gaps, while a 0 % cloud cover means a completely clear sky. The impact on cloud cover is influenced by various atmospheric processes and conditions, including water vapor content, temperature, air masses, and local topography. Factors such as atmospheric instability, convergence of air masses, and lifting processes, like orographic lifting over mountains, contribute to cloud formation and dispersion.

The various kinds of clouds that make up the atmosphere are the reason for the variation in cloud cover. Based on their appearance and altitude, clouds are classified into three main categories:

1.High-level clouds, like cirrus and cirrostratus, form at elevations above 6100 meters and consist mainly of ice crystals. Cirrus clouds appear as thin, feathery wisps or long, thread-like patterns that stretch across the sky. They often align parallel to the jet stream and can occur individually or in scattered patches. In astronomy, cirrus clouds can interfere with ground-based observations of celestial objects. Their presence can cause distorted images and reduce image quality, affecting the clarity of astronomical observations.

2.Mid-level clouds, such as altocumulus and altostratus, form at altitudes between 2000 to 6100 meters and consist of a mix of water droplets and ice crystals. These clouds often appear as spherical, puffy masses or extended rolls, and they frequently cover the sky in distinct rows or patches.

3.Low-level clouds like stratus and cumulus form below 2000 meters and are predominantly composed of water droplets. Since these clouds are commonly found at lower altitudes, they are not as crucial for our purposes in astronomy when using telescopes to study and observe. [18]

2.7. Vertical aerosol optical depth

Vertical Aerosol Optical Depth, abbreviated as VAOD is a very important parameter for this study, because we used it to correlate the MAGIC LIDAR telescope and CTA FRAM. Aerosols in the atmosphere, which are made up of a wide variety of suspended particles, have a substantial impact on climate, weather, and air quality. Accurate parameters are required to evaluate the geographical distribution of aerosols and how they interact with solar radiation. The vertical distribution of aerosols is not included in the Aerosol Optical Depth (AOD), which describes the overall attenuation of solar radiation throughout the whole atmospheric column. This makes the Vertical Aerosol Optical Depth (VAOD) an important metric that provides a thorough understanding of aerosol behavior at various altitudes. AOD and VAOD differ in that AOD uses data between 0 and 1 whereas VAOD uses data above 0. We have a thicker layer of aerosol, generally clouds, if the VAOD value is greater. [9]

We will now go over the measurement process for VAOD. Utilizing a variety of methods and tools, measuring Vertical Aerosol Optical Depth (VAOD) entails determining the aerosol optical depth inside particular atmospheric layers. These methods rely on data from devices that are either ground-based, airborne, or satellite-borne, each with their own advantages and disadvantages. The first method is Sun photometry, also known as sun photometer measurements. This approach involves using specialized equipment called sun photometers to observe the Sun's direct solar energy at various wavelengths. The sun photometers are carefully calibrated to accurately measure the Sun's brightness. Measurements are typically taken under clear skies and at various solar zenith angles. By analyzing the data obtained from these measurements, researchers can gain valuable insights into the presence and characteristics of aerosols in the atmosphere. The aerosol optical depth (AOD) at each wavelength is then determined using the observed spectral data. Radiative transfer models and inversion procedures are used to estimate VAOD. These models compute the vertical distribution of aerosols and create VAOD profiles within certain atmospheric layers by taking into account the characteristics of the environment, such as pressure, temperature, and particle size distribution.

LIDAR (Light Detection And Ranging) is the second technique, which we shall go into more depth about later. Lidar is a type of remote sensing that employs laser pulses to scan the atmosphere and get precise vertical aerosol profiles. The backscattered laser light from aerosol particles is measured using sensitive detectors and telescopes on lidar devices, which are used to assess VAOD.

Lidar offers high-resolution data on the scattering characteristics of aerosols that are dependent on height. The Aerosol Optical Depth inside each atmospheric layer may be determined by integrating the backscattered signals across certain atmospheric layers, yielding VAOD values.

In-situ measurements and satellite remote sensing are the other two methods. Remote sensing-capable satellite-borne devices have completely changed how we can track aerosols on a global basis. AOD data is available from instruments like CALIPSO (Cloud-Aerosol Lidar and Infrared Pathfinder Satellite Observation) and MODIS (Moderate Resolution Imaging Spectroradiometer).

Advanced retrieval techniques and data assimilation methods are employed to infer vertical aerosol dispersion and obtain VAOD estimations even though these satellite sensors

naturally measure column-integrated AOD. These methods rely on a mix of multi-spectral observations, lidar data, and advanced algorithms. In-situ measurements use specialized sensors mounted on airplanes or research balloons to directly sample aerosol particles at various altitudes. Aerosol particle counts, nephelometers, and mass spectrometers are a few examples of these tools. Researchers can estimate VAOD values within constrained vertical layers thanks to the extensive knowledge on aerosol characteristics provided by in-situ measurements at particular locations and altitudes.

Scientists frequently combine complimentary data from several methodologies and sensors to increase the precision and dependability of VAOD measurements. For instance, data assimilation can be used to integrate sun photometer readings with LIDAR observations or satellite data in order to further restrict the vertical distribution of aerosols and improve VAOD estimations.

Other difference between AOD and VAOD is in calculation. AOD is obtained from precise observations of the Sun, as we previously said. AOD estimates must account for Rayleigh scattering, which is the scattering of sunlight by air molecules without the participation of particles, even with well calibrated sensors. In order to isolate the aerosol scattering impact, this modification is necessary. The AOD at each wavelength is derived after the sun photometer values have been calibrated and adjusted for Rayleigh scattering. The aerosol loading in the atmosphere is then described using the AOD values.

The initial step in calculating VAOD is to acquire Aerosol Optical Depth (AOD) readings using satellite-based equipment or solar photometry. The integrated aerosol loading along the air column is represented by these AOD data. Researchers use radiative transfer models, which imitate how solar radiation interacts with the atmosphere, to determine VAOD. These models take into consideration aspects of the atmosphere such pressure, temperature, the size distribution of the aerosols, and their vertical distribution. Inversion methods are used to invert the vertical information and create VAOD profiles using the observed AOD and radiative transfer models. In order to match the measured AOD values, these algorithms find out the vertical aerosol distribution that fits the data the best. Techniques for data assimilation can be used when only column-integrated AOD data is available (for example, from satellite sensors). These methods use data from several sources to infer vertical aerosol information and enhance VAOD estimations, such as LIDAR measurements or other remote sensing data. A collection of vertical profiles that

characterize the aerosol optical depth within predetermined atmospheric layers are the result of the VAOD computation. These profiles shed light on the scattering and concentration characteristics of aerosols at various altitudes.

It is important to note that measuring VAOD is more difficult than measuring AOD since it needs more equipment and better modeling methods. The efficacy of the radiative transfer and inversion methods employed in the study, as well as the quality and availability of vertical aerosol data, all influence the accuracy of VAOD estimations.

By considering these crucial atmospheric parameters we can gain deeper insights into the underlaying mechanisms responsible for the changes in our weather and additionally, on which essential factors we have to pay attention in astronomy before we start some observations.

3. INSTRUMENTS FOR ATMOSPHERIC CARACTERIZATION

In this paragraph, we will explain the formation of cosmic showers, Cherenkov radiation, and why they are important to us. We will also describe the atmosphere above the Canary Islands and how LIDAR and FRAM work.

Air shower formation in the atmosphere is an intricate and interesting phenomenon that is essential for the study of high-energy astrophysics and has significant implications for comprehending extreme phenomena in space. This subject contains a number of important components that together improve our understanding of the universe's high-energy processes. In order to determine the origins of high-energy particles in space, scientists might first use the examination of air shower development. This includes pulsars, supernova remnants, and active galactic nuclei, giving us a greater knowledge of the characteristics of these objects and their function in cosmic processes. It also makes it possible to better understand the properties of high-energy particles, including their energy, velocity, and composition.

Air density, pressure, and temperature are important atmospheric factors that affect how an air shower develops. Understanding their impact makes it possible to analyze high-energy particles' penetration into the atmosphere with more accuracy, providing important information about how they interact with the environment. As the depth of atmospheric entry increases, more high-energy particles interact with atmospheric atoms and molecules, making air density particularly important. Secondary particle formation is enhanced as a result of the increased contact. Due to numerous collisions with atoms and molecules, the dense atmosphere also plays a role in the rapid energy losses of high-energy particles, which slow them down as they travel through the atmosphere.

Cosmic air showers development is also influenced by atmospheric pressure. Higher air density and lower pressure at higher altitudes result in fewer interactions between high-energy particles and atmospheric particles. This may have an impact on the air shower's structure and the depth at which particles enter the atmosphere.

The velocity of particles in the atmosphere is influenced by temperature, which also has an impact. Higher temperatures cause air molecules to move more quickly, which can change how quickly and how long high-energy particles interact with them.

When analyzing the formation of an air shower, all these changing atmospheric factors must be taken into consideration. In order to simulate and study the properties of the air shower, including its depth of penetration into the atmosphere, form, and Cherenkov radiation propagation, scientists must have an extensive understanding of these aspects.

Research into air showers and high-energy astrophysics can also further our knowledge of dark matter. According to hypotheses, high-energy particles from dark matter could be able to interact with visible matter. It is possible to find proof of the presence of dark matter in the cosmos by following these particles and associated air showers, which would be a big development for astronomy and particle physics. [5]

We can now see that high-energy cosmic particles reach Earth's atmosphere with a lot of kinetic energy as we look more into the process of air shower production in the atmosphere. Secondary particles such charged pions and kaons are produced as a result of interactions this energy starts with air atoms and molecules. These secondary particles continue to disintegrate and produce new particles as they do so. They have a finite shelf life.

As they travel through the atmosphere, these secondary particles collide with other atoms and molecules, losing energy in the process. The speed of secondary particles steadily decreases as they move through the atmosphere as a result of this energy loss process, known as energy loss by ionization.

When secondary particle speed goes below the speed of light in the atmosphere, an essential point in air shower production is reached. At this time, electromagnetic radiation in the visible and near-ultraviolet regions of the spectrum, known as Cherenkov radiation, is released. This radiation generally has a blue hue and spreads in a cone-shaped pattern along the direction of the main particle's travel.

Cherenkov telescopes are used to find and examine this Cherenkov radiation. Cherenkov radiation is captured by these telescopes' reflectors, which are frequently parabola-shaped and used to focus it onto detecting surfaces. These surfaces are covered with extremely sensitive photomultiplier tubes, which turn the light photons from Cherenkov radiation into electrical impulses. Detection of a cosmic shower is illustrated in *Figure 3*.

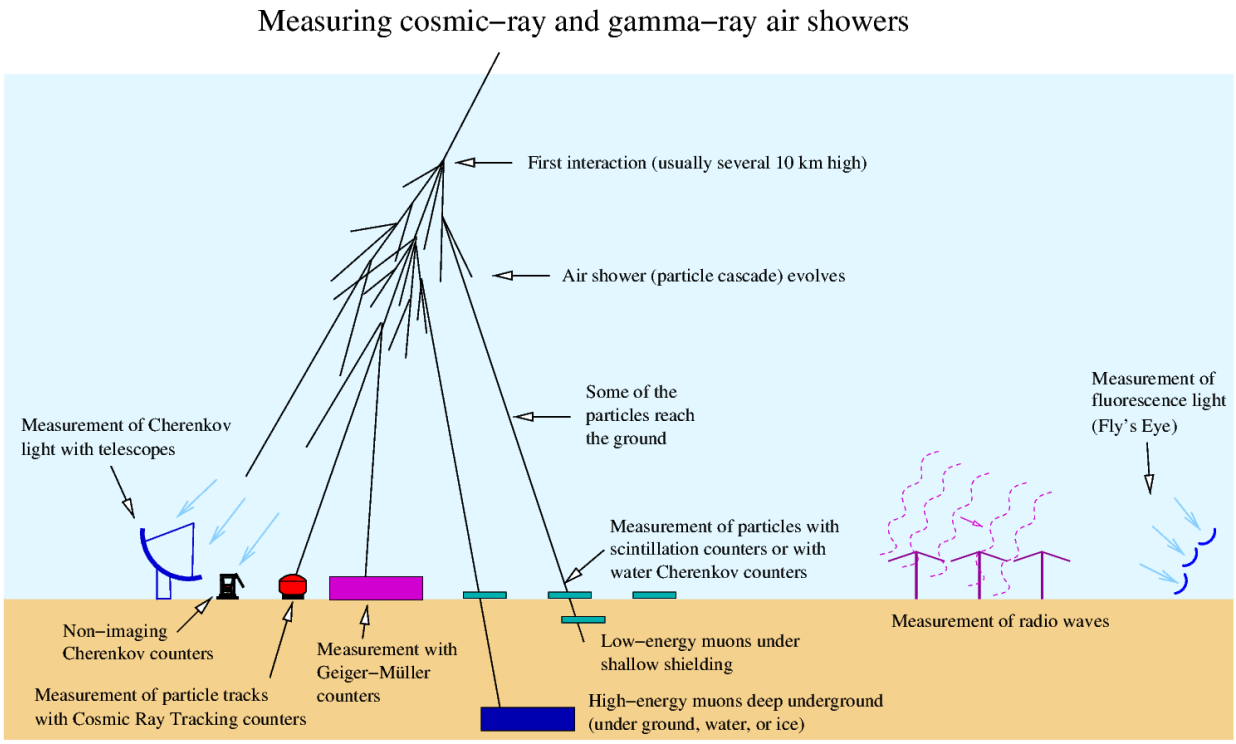

Figure 3. Detection of cosmic air showers [3]

Scientists may recreate the properties of the air shower, including the energy, velocity, and direction of the source cosmic particles that caused the Cherenkov radiation, by analyzing the data gathered from these telescopes. These telescopes, which are essential for advancing our knowledge of high-energy astrophysics and advancing the investigation of extreme processes in space, include VERITAS (Very Energetic Radiation Imaging Telescope Array System), H.E.S.S. (High Energy Stereoscopic System), and MAGIC (Major Atmospheric Gamma Imaging Cherenkov).

3.1. Atmosphere above Canary Islands

The Canary Islands are an archipelago situated in the Atlantic Ocean west of the North African coast approximately 18-13° W, 27 – 29° N. It consists of seven islands, namely El Hierro, La Palma, La Gomera, Tenerife, Gran Canaria, Fuerteventura and Lanzarote. The islands are of volcanic origin and have extremely complicated, steep topography, which results in a high vertical range that varies with their age. The islands have a subtropical climate with mild air temperatures all year round. Mild winters with mean air temperatures above 20 °C, low precipitation (225 millimetres per year on average; east islands are desert with over than 100 mm per year) and high sunshine, more than 2800 hours per year. On Tenerife, Mount Teide (3718 m) is the highest point. [1]

The highest peaks on La Palma, Gran Canaria, La Gomera, and El Hierro, which together make up a midsize cluster, are 2423 meters high. Although the North Atlantic Oscillation has an impact, the Canary Islands' climate is often fairly steady and dry thanks to the influence of the trade winds. The trade winds are strongest during the winter and when the Arctic oscillation is in its warm phase, and they primarily originate from the northeast in the Northern Hemisphere and the southeast in the Southern Hemisphere. The vertical stratification shows a typical structure with three layers. Above a subsidence inversion is found up to about 1500 m, resulting from the downwelling flow of the Hadley cell. The Hadley cell, also referred to as the Hadley circulation, is a tropical atmospheric circulation that occurs on a large scale across the entire planet. It is characterized by air rising close to the equator, flowing poleward near the tropopause at a height of 12–15 km above the Earth's surface, cooling and descending in the subtropics at about 25 degrees latitude, and then returning close to the equator. This layer's overall temperature increase effectively prohibits any convection and, as a result, the movement of water vapor to higher altitudes. As a result, water vapor condenses below the inversion layer to form "sea of clouds"—thin stratocumulus clouds that are normally nonprecipitating. [10] Normally, the cloud layer is between 1200 and 1600 meters high, but in July and August, it frequently drops to 800-1000 meters. Additionally, during dust outbreak events from the Sahara, known as Calima on the Canary Islands, the vertical stratification might disappear under hot air invasions. [1]

An "Alisio" inversion occurs whenever the temperature inversion is able to distinguish between two clearly defined regimes: the wet marine boundary layer (MBL) and the dry free troposphere (FT) above it. Inversion of the "Alisio" occurs roughly 80% of the time. [10] These incursions, which occur more frequently in the winter and less frequently in the spring, cause a rise in temperature and a drop in hygrometric values, a predominant easterly wind, a stable environment, and reduced visibility due to airborne dust. Depending on where they come from, which could be the Atlantic Ocean, the Sahara Desert, or Europe, dust particles are classified as marine, desert, or anthropogenic aerosols. The Archipelago has a wide range of diverse climates as a result of the vast vertical range and associated variances in temperature and precipitation. The sea of clouds can definitely be seen for Tenerife and La Palma in the areas below the inversion layer, even if the peaks of Tenerife and La Palma are practically completely cloud-free. The free troposphere can be described as "ultra-clean" under these circumstances. The Canarian observatories are situated between 2100 m and 2400 m because of the clear atmospheric conditions, which is one of the main causes. For Gran Canaria, El Hierro, and La Gomera the cloud occurrence is much higher at the windward northern sectors. [1]

3.2. MAGIC LIDAR

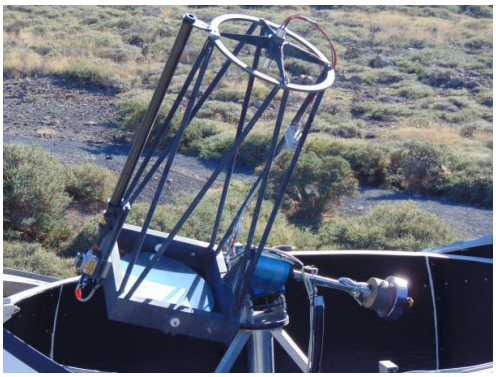

Figure 4. MAGIC LIDAR [8]

In contemporary atmospheric research, remote-sensing techniques have become essential, and among them is Light Detection and Ranging (LIDAR) which play crucial roles in the profiling of the atmosphere. Lidar provide high spatial and temporal resolution measurements, allowing researchers to observe the atmosphere under ambient conditions. Additionally, lidar instruments have the advantage of covering the height range from ground level up to more than 100 km altitude, making them attractive tools for atmospheric studies.

LIDAR versatility lies in its ability to interact with various atmospheric constituents, enabling the determination of fundamental atmospheric variables such as temperature, pressure, humidity and wind. Moreover, LIDAR can measure aerosols and clouds, providing valuable insights into atmospheric composition and processes. In cloud studies, lidar distinguishes between water droplets and ice crystals and contributes to understanding the climatic effects of aerosols.

Beyond cloud and aerosol research, LIDAR is a powerful tool for monitoring air pollution, desert dust and smoke from forest fires over vast distances. It can trace the transport of these airborne particles across continents, helping to understand their dispersion patterns and potential effects on air quality and climate on a global scale.

Over the past decades, lidar has significantly contributed to our understanding of the Earth's atmosphere, especially regarding highly variable atmospheric parameters. It is particularly useful for studying processes on various scales, from a few cubic meters and seconds to global, multi-year coverage. [15]

3.2.1. Lidar setup

The LIDAR apparatus is securely housed within a protective dome situated above the LIDAR control room atop the MAGIC control building. This control building accommodates the computing infrastructure and electronic components essential for the functioning of the MAGIC telescopes. The primary objective of the LIDAR system is to perform real-time monitoring of the atmospheric extinction profile across the observed field-of-view during the nightly observations conducted by the MAGIC telescopes. For this purpose, we utilize a micro-Joule LIDAR system operational at a wavelength of 532 nm.

Figure 5. shows an illustration of the LIDAR configuration with its key hardware components.

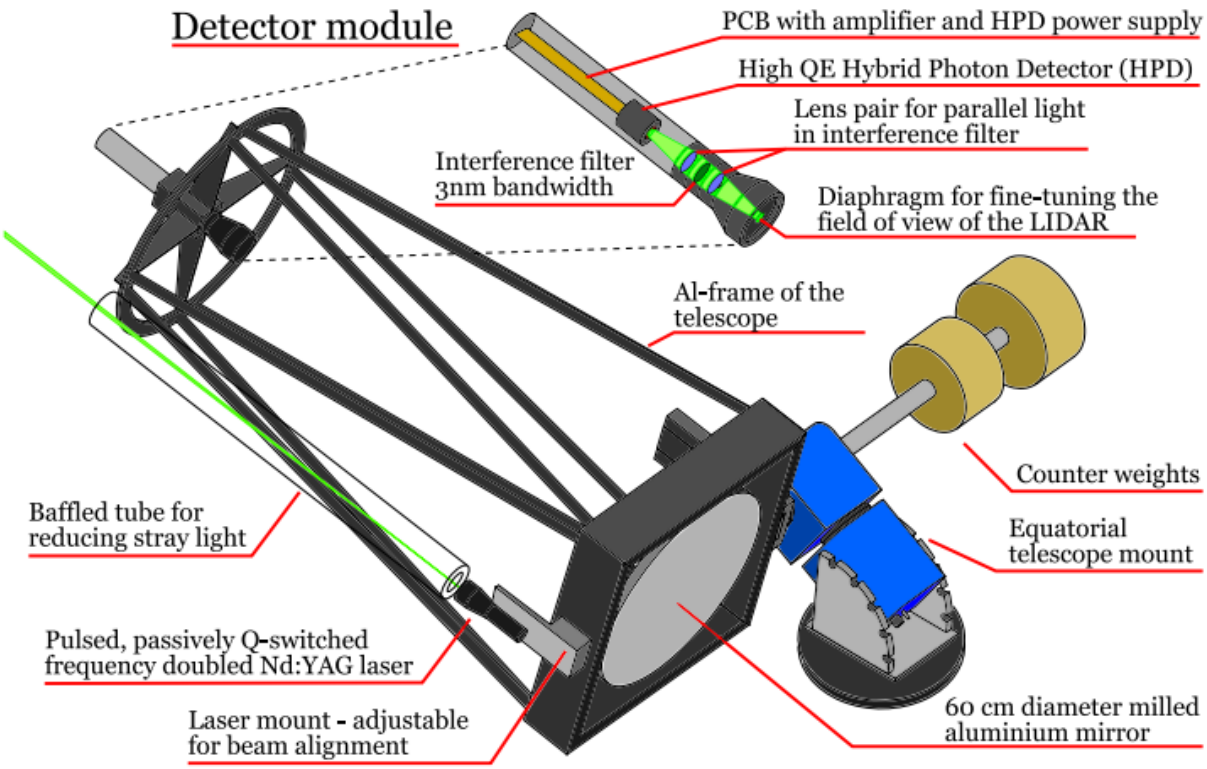

Figure 5. Hardware components of the MAGIC LIDAR [10]

The Nd:YAG laser used in the LIDAR is frequency-doubled, pulsed, passively Q-switched, with pulse energies of 5 J (25 J) and 300 Hz (250 Hz), respectively. A photodiode built within the laser is utilized to externally trigger the readout. The beam divergence is decreased to 10 mrad (12 mrad) using a 10 mrad (20 mrad) beam expander. The LIDAR telescope and detector are installed on a

specially made assembly that makes it possible to coordinate the laser setup with them quickly and precisely.

Positioned directly ahead of the laser, the beam expander is thoughtfully spaced to considerably curtail beam divergence. However, dust particles present on the exit window of the expander might cause a slight portion of the laser light to scatter away from the beam. This dispersed light could possibly travel toward the LIDAR detector; nonetheless, it avoids overwhelming the detector and can subsequently be excluded using data based on its initial arrival time.

On the recipient end, an off-axis arrangement relative to the emitter is employed, utilizing a substantial aluminum mirror measuring 60 cm and featuring a diamond-milled surface. This mirror has a focal distance of 150 cm. In the mirror's focal plane, the detector optics incorporate an aperture diaphragm, which is adjusted to approximately 6 mm in diameter. A diminutive telescope, comprising a pair of lenses, captures an image of the diaphragm and projects it onto the surface of the Hybrid Photo Detector (HPD), thereby constraining the accepted solid angles.

A 3 nm bandwidth interference (IF) filter situated between the lenses is used to choose the wavelength. It is beneficial to dim the light of the night sky (LoNS) by a factor of at least 100. After the narrow band filter, a second lens with over 50% quantum efficiency (QE) at 532 nm maps the light onto the photo-cathode of a hybrid photo detector (HPD). [10]

3.2.2. LIDAR data

The LIDAR is controlled through a graphical user interface written in LabVIEW. Two distinct photon counting techniques are applied to the raw data when a LIDAR shot sequence is complete, and the raw data is then promptly erased to conserve disk space. Finding single photon-electron peaks is the goal of the first "photon counting" algorithm. The second "analogue" procedure takes the waveform's integral and divides it by the single photon's mean charge, which is calculated from the distribution of single photon charge integrals from the same data sample. Due to the superior charge resolution of the used HPD, single photo-electron waveform integration is feasible. [8]

However, the two underlying presumptions that underpin the correction of MAGIC scientific data for aerosols and clouds in its field of view are as follows:

(i) The nighttime boundary layer is often located below the Cherenkov light emission height typically seen by the MAGIC Telescopes during gamma-ray shower

observations, but its structure does not need to be resolved, only its overall transmission counts.

(ii) In comparison to normal longitudinal shower profiles, which cover several kilometers, the great majority of layers at higher elevations can be thin. Therefore, it is not necessary to determine their internal structure either; just the cloud layer's overall transmission.

Because of that, a good resolution is not necessary. Instead, quality criteria include a good transmission resolution for optically thin aerosol and cloud layers. [10]

In the following figure (*Figure 6.*), the obtained LIDAR data and an example of their analysis are presented. The resulting graphs depict the dependence of photon count on distance from the detector. The return signal is corrected by the spatial angle multiplied by R^2 and the logarithm of that product. Here, R represents the distance from the scattering region. The reason for the logarithmic correction is that the photon count exponentially decreases with distance. Furthermore, uncertainties and errors are not shown on the graphs to keep them visually cleaner. For instance, for larger distances, in this graph above 12000 m, we observe noise that vividly demonstrates errors. Naturally, when calculating the data needed for further analysis and research, errors are taken into account.

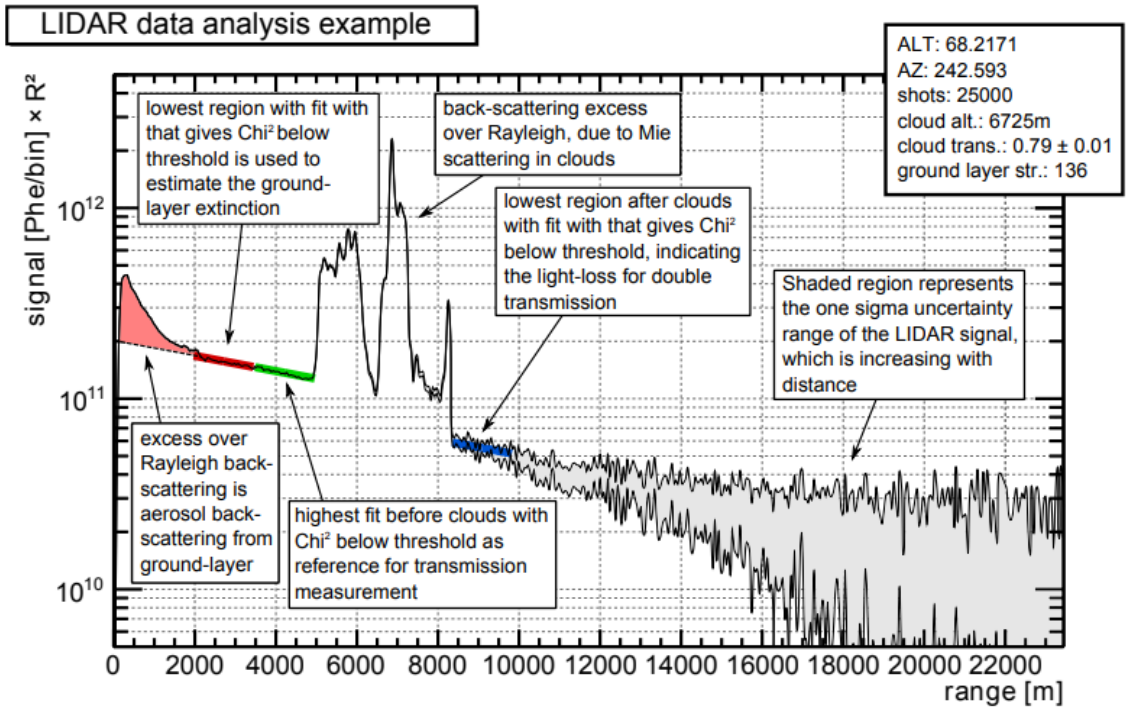

Figure 6. LIDAR data analysis example [11]

In the first few hundred meters, we can observe a sharp increase in photon count, from 0 to 10^{11}. This rapid rise is attributed to the misalignment of the detector and the laser off the axis. Another contributing factor is that the backscattered light is detected only within the field of view of the detector after the pulse has traveled a certain distance. In the initial kilometers, we notice a decrease in photon count, which is related to the planetary boundary layer, i.e., the lowest layer of the atmosphere. After this decrease, we observe a linear decline in photon count, attributed to Rayleigh scattering interactions.

Fitting the Rayleigh scattering interaction is a highly complex process due to dependencies on temperature, air pressure, air density, etc. Above 5000 meters, we can observe high peaks resulting from cloud presence at those altitudes. Following the peaks, we again see linear behavior, though not the same function as before the peaks. Notably, the intercept on the Y-axis is smaller due to the amount of light lost within the cloud.

Comparing the graph before and after the peaks provides insights into light transmission within that region. The transmission coefficient is a measure that indicates how much light passes through a medium, in this case, the atmosphere, without being absorbed or scattered. It's often expressed as a percentage or a number between 0 and 1, where 0 signifies no transmission and 1 complete transmission. In the context of aerosols, the transmission coefficient describes the ratio of light that can pass through the atmosphere in relation to the presence of aerosol particles.

In the final kilometers, obtaining reliable data is challenging due to significant noise, evident in the graph. Notably, uncertainties increase as distance, i.e., altitude, increases.

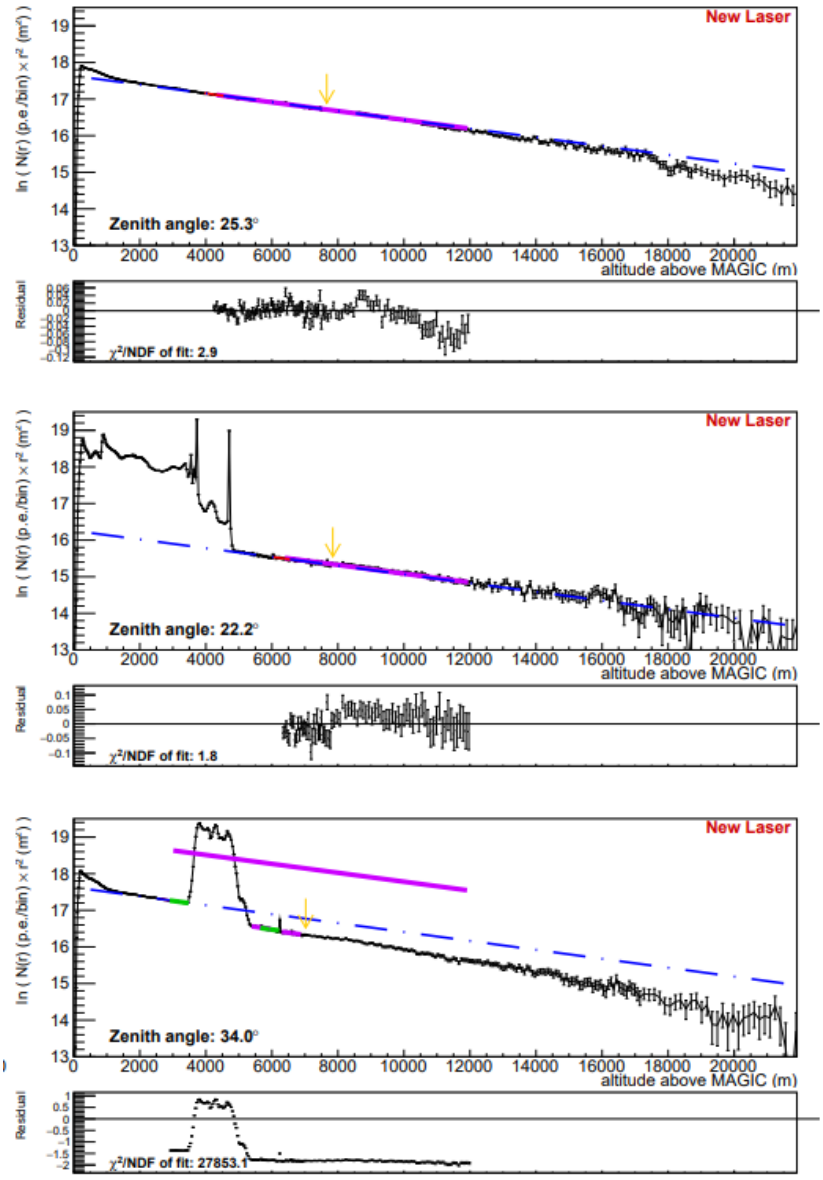

Figure 7. Example for LIDAR date during clear night (top), nights with calima (middle) and nights with clouds (bottom) [10]

In *Figure 7.* the fitted measurements from the LIDAR are presented. The first image illustrates a clear sky, devoid of cloud presence, the middle image depicts conditions during calima, and the bottom image showcases measurements taken under cloud presence. The green fits represent Rayleigh scattering. When comparing the upper image with the remaining two, it's evident that throughout the graph, the photon count experiences linear decline without the presence of peaks.

The middle image displays peaks up to 5000 meters, indicating the presence of clouds up to that altitude—a characteristic feature of calima, a desert wind carrying sand and dust. The final image

demonstrates cloud presence at altitudes ranging from 4000 to 6000 meters. Moreover, there's a noticeable difference in the intercept on the Y-axis before and after the peaks, which signifies cloud presence. This distinction enables the calculation of the transmittance coefficient.

For calculating the transmittance coefficient, we require the detected signal within the Rayleigh region, which can be expressed as:

$$N(r) \cdot r^2 \simeq exp\,(C - s \cdot r) \tag{1}$$

Where *N(r)* is the return signal, and *C* and *s* are constants. Here, C represents the intercept on the Y-axis, and s denotes the slope coefficient. More precisely, the Y-axis values on the graph are logarithmic, so the equation of the line we have is:

$$\ln(N(r) \cdot r^2) \simeq C - s \cdot r \tag{2}$$

From this equation, we deduce that we have the equation of a line, where *C* is the Y-axis intercept, and *s* is the slope coefficient.

Directly obtaining information about transmittance from the scattered light is challenging due to LIDAR operating at a single wavelength. Transmittance values can be acquired by comparing photon counts at two distinct altitudes. When fitting data at altitudes r_1 and r_2, the slope coefficient *s* should remain constant, only the intercept *C* changes. Thus, we introduce constants C_1 and C_2. The difference in the number of detected photons can be expressed as an exponential function:

$$\exp\big(-(C_1 - C_1)\big) \tag{3}$$

Hence, we know the relative photon count at altitude r_2 in relation to altitude r_1. This value essentially represents the signal attenuation due to double transmittance. Since the laser beam passes through the same atmospheric layer twice—once while going up and again while returning—we encounter double transmittance. Consequently, the transmittance coefficient needs to be adjusted accordingly. The final formula for calculating the transmittance coefficient is:

$$T_{1,2} = \exp(-\tfrac{1}{2}(C_1 - C_1)) \tag{4}$$

The link between transmittance and VAOD lies in their common description of light behavior in interaction with aerosols. Moreover, we can establish a connection between them using the formula:

$$T = e^{-VAOD} \tag{5}$$

where 'e' is the base of the natural logarithm

According to this equation, the transmission coefficient drops down exponentially as VAOD rises. In other words, a lower transmission coefficient is caused by more light being scattered and absorbed as the aerosol concentration (VAOD) in the atmosphere rises.

We have to be aware that this connection may be oversimplified since atmospheric interactions can be complicated depending on the composition, size distribution, and atmospheric circumstances of the aerosols. To give a rough idea of how these two ideas connect in the context of aerosol optics, consider the relationship indicated above.

3.3. FRAM

A FRAM (F/(Ph)otometric Robotic Atmospheric Monitor) telescope is a sophisticated system comprising a robotic mount, a large-format CCD camera, and a fast telephoto lens. Its primary purpose is to monitor atmospheric conditions at any location where accurate information about atmospheric transparency is required. The FRAM telescope excels in providing high spatial or temporal resolution data, especially in situations where continuous use of laser-based methods might interfere with other observations.

3.3.1. FRAM setup

The FRAM setup consists of two instruments: a small astronomical telescope and a telephoto lens, both outfitted with a CCD camera. Both of these instruments are mounted on a single equatorial mount, which can track a 2 minutes exposure on the equator with the main telescope's 2-meter effective focal length.

The main telescope is around 30 cm equipped with a focal reducer and a micro-focuser. The light from the telescope is collected by a CCD camera which translates to 23 x 15 arcmins of fields of view. On top of the telescope, a wide-field camera is mounted, which consists of a photographic lens. Additional equipment includes an external filter wheel with photometric filters. All the equipment is housed in a custom-built dome which is opened and closed using a hydraulic pump controlled by a computer. [14,12]

Figure 8. The FRAM [8]

3.3.2. VAOD measuring

The transparency of the atmosphere above the sites is monitored using the FRAM telescopes and LIDAR. The difference between FRAM and LIDAR is that the first instrument provides only the integral value of the vertical aerosol optical depth (VAOD) through the whole atmosphere, while whole LIDAR measures the whole vertical profile. Now, we will briefly describe how FRAM measures VAOD.

FRAM uses the interaction of solar radiation with suspended aerosol particles, operating at its heart on the concept of sun photometry. Through this interaction, FRAM learns crucial information about the optical characteristics of aerosols, enabling the measurement of vertical aerosol optical depth (VAOD).

A fundamental device essential to the data collecting process, is the multi-filter radiometer. This radiometer is meticulously constructed to collect sunlight at many distinct wavelengths, each of which is closely associated with particular aerosol properties. The radiometer's capacity to distinguish between various wavelength-dependent characteristics enables FRAM to unravel the complex optical patterns identifying the components of atmospheric aerosols.

FRAM follows a strict calibration methodology in its quest of data precision and accuracy. Signal records are carefully synchronized with reference measurements taken under precisely defined air conditions throughout this calibration procedure. By converting unquantified readings into quantifiable units of aerosol optical depth, this calibration creates a key connection between the data that has been collected and the physicochemical characteristics of the aerosol-filled

atmospheric environment. After a successful calibration Aerosol optical depth (AOD), a crucial metric in aerosol investigations, is determined from the radiometer's data.

However, applying advanced inversion techniques is a necessary step in the process of determining VAOD. These methods rely on radiative transfer calculations, atmospheric models, auxiliary data, and vertical temperature and pressure profiles. These elements come together to provide a vertical profile that reveals the distribution of aerosol concentration at various altitudes.

The combination of aerosol concentration data across distinct height segments encapsulates the core of VAOD. The vertical aerosol optical depth, which represents aerosol effect within various atmospheric strata, is the result of this merger. VAOD provides a sophisticated representation of aerosol spatiotemporal dynamics by including the full range of aerosol interactions at distinct altitudinal levels. In *Figure 8.* measurements of VAOD over time are shown. The same color of data corresponds to measurements taken on the same day. [13]

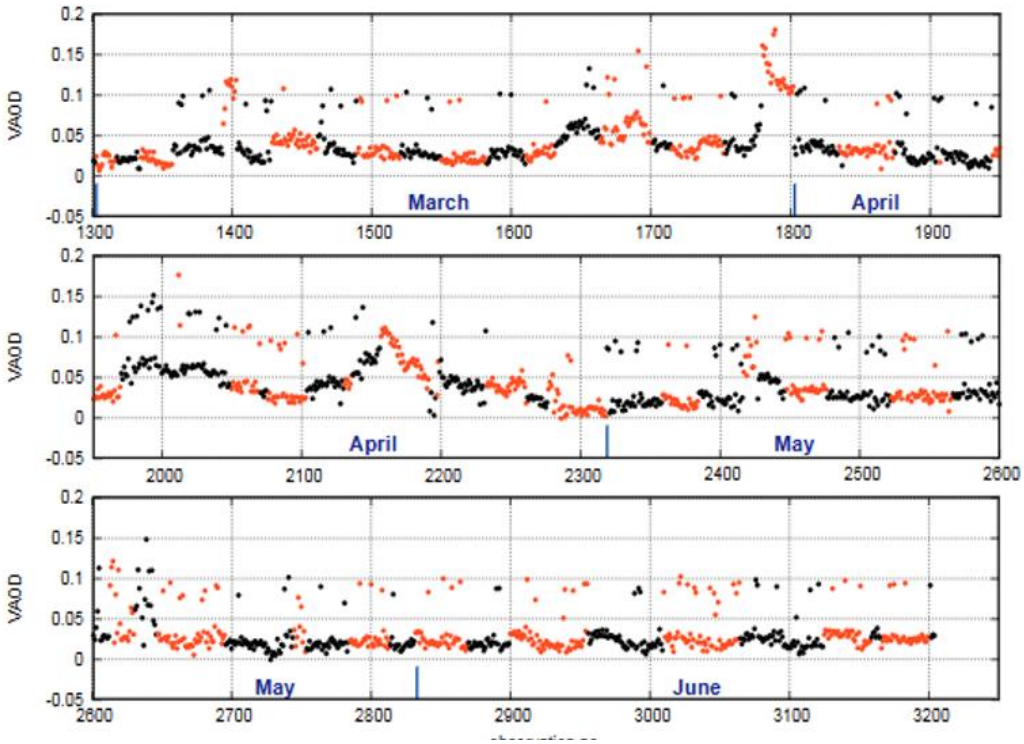

Figure 9. VAOD data measured with FRAM [13]

4. FRAM AND LIDAR VAOD CORRELATION

4.1. Motivation behind the correlation of MAGIC LIDAR and CTA FRAM

As previously indicated, vertical optical depth (VAOD) serves as a gauge for assessing the extent to which light can traverse the atmosphere during celestial observations. The measurement of VAOD holds paramount importance in the realm of astronomy due to the pivotal role the atmosphere plays in distorting incoming spaceborne light. The fusion of LIDAR and FRAM telescopes in gauging VAOD yields invaluable insights into atmospheric impacts and facilitates rectifications of these effects, leading to more finely tuned astronomical observations.

The measurement of VAOD assumes significance in light of its capacity to offer a lucid grasp of the degree to which the atmosphere influences light's passage through varying atmospheric strata. Additionally, VAOD measurements empower astronomers with an understanding of how atmospheric influences modulate the intensity of incoming space-derived light. These measurements form the basis for corrections that offset light distortions, particularly crucial when observing variable entities whose luminosity undergoes fluctuations over temporal spans.

Moreover, the pertinence of VAOD measurements extends to optimizing the scheduling of observation sessions. By utilizing LIDAR for VAOD measurements, astronomers can cherry-pick time intervals characterized by diminished atmospheric turbulence, resulting in diminished light distortion due to atmospheric interaction. The optimization of observations further bolsters the resource-efficient utilization of telescopic facilities and related assets. Operating under prime conditions characterized by lower VAOD, the likelihood of observations being swayed by atmospheric impacts is curtailed. This translates to a higher proportion of beneficial and top-tier quality observations, which in turn trims the necessity for repetitive observations of identical objects. Notably, high-caliber and fine-tuned observations empower astronomers with a higher caliber of results and a more profound comprehension of scrutinized phenomena. This is evident in the precision of light curves, which are subjected to less atmospheric distortion, facilitating superior analysis and interpretation of flux alterations within celestial objects, and fostering an enhanced grasp of their intrinsic makeup and developmental trajectories.

In essence, LIDAR systems harness the core tenet of laser illumination to glean intricate insights into atmospheric attributes. These apparatuses emit laser beams into the atmospheric expanse and chronicle the elapsed time for light to bounce back onto sensors. This procedural methodology underpins the assessment of altitudes and densities encompassing distinct atmospheric strata. By

amalgamating this dataset, a tridimensional portrayal of the atmospheric framework takes shape. On a contrasting note, the FRAM telescope, distinguished by its exceptional sensitivity and rapid image capture rates, affords the capacity to track swift flux fluctuations within celestial entities. This facet assumes paramount importance when elucidating changes oftentimes entwined with atmospheric ramifications, including turbulence and light diffraction. The accelerated flux alterations frequently unearth insights about celestial subjects that would otherwise succumb to atmospheric distortions.

The amalgamation of data sourced from LIDAR and FRAM telescopes empowers astronomers to dissect and pinpoint patterns of congruence between atmospheric influences and flux dynamics. This correlation lends a hand in deciphering how atmospheric conditions impinge upon flux dynamics and how these influences manifest within dataset constructs. This phase paves the way for the formulation of mathematical models that quantify the linkage between vertical optical depth (VAOD) and oscillations in luminosity. By leveraging VAOD measurements as a foundational premise, corrections can be devised to counterbalance atmospheric consequences that distort luminosity curves as gauged by the FRAM telescope. These corrective interventions are pivotal in elevating data quality standards. Elevated luminosity curves and image precision equip astronomers to conduct more nuanced analyses, deepen the comprehension of luminosity shifts, and refine the understanding of the intrinsic characteristics of the celestial entities under scrutiny.

In summation, the harmonious amalgamation of LIDAR and FRAM telescopes ushers in a holistic methodology for comprehending the atmospheric underpinnings of observations, while concurrently enabling the rectifications that elevate the caliber and dependability of data acquisitions. This symbiotic partnership contributes to heightened precision in analyses and an enriched appreciation of the tapestry of celestial phenomena.

4.2. Correlation procedure

In this section, we will present the correlation between LIDAR VAOD values and FRAM VAOD values, as well as their correlation. As we explained earlier, the correlation between these two devices is crucial for further research.

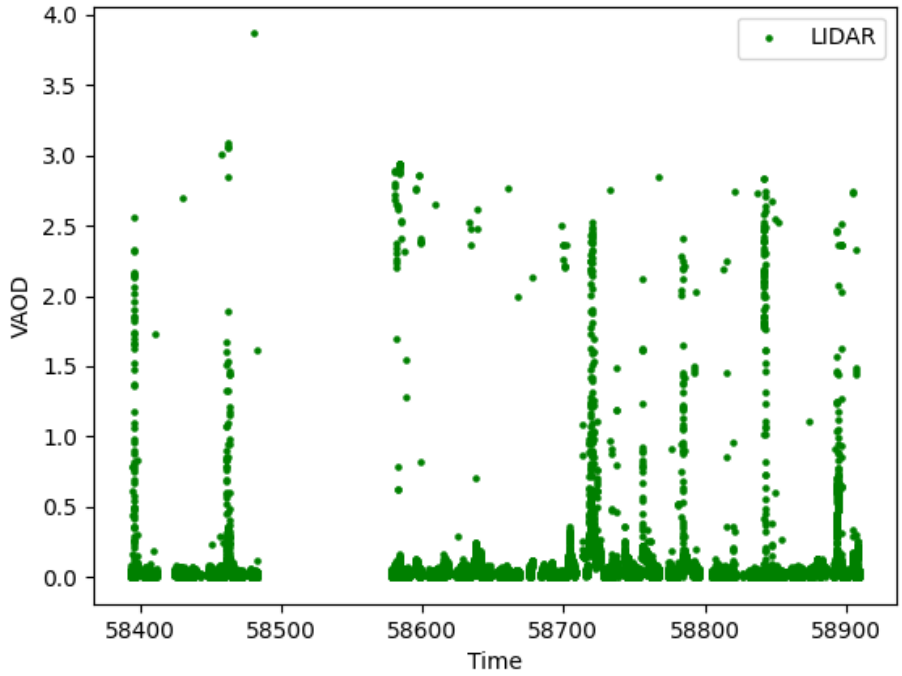

Figure 10. Variations of LIDAR VAOD over time

Figure 10.. illustrates the dependence of VAOD over time measured with MAGIC LIDAR. The measurements were conducted in the time period from 1. October 2018, to 1. March, 2020. Through a detailed analysis of the data, we observed irregularities, e.g., some VAOD values were negative, which is impossible, so we excluded those values from the presentation and calculations. Negative VAOD values likely resulted from imperfections in the device and the potential for irregularities. Additionally, very high VAOD values appeared that were not connected to the rest of the values. By examining the MAGIC Runbook, which outlines technical issues, it became evident that during that period, MAGIC LIDAR encountered problems and its operation was not consistent.

Upon observing the graph, it's also noticeable that we don't have all the VAOD values. Specifically, due to technical problems, MAGIC LIDAR was unable to perform measurements. The graph in *Figure 10*. excellently displays the fluctuations in VAOD values. We observe several peaks indicating high VAOD, hence the presence of clouds.

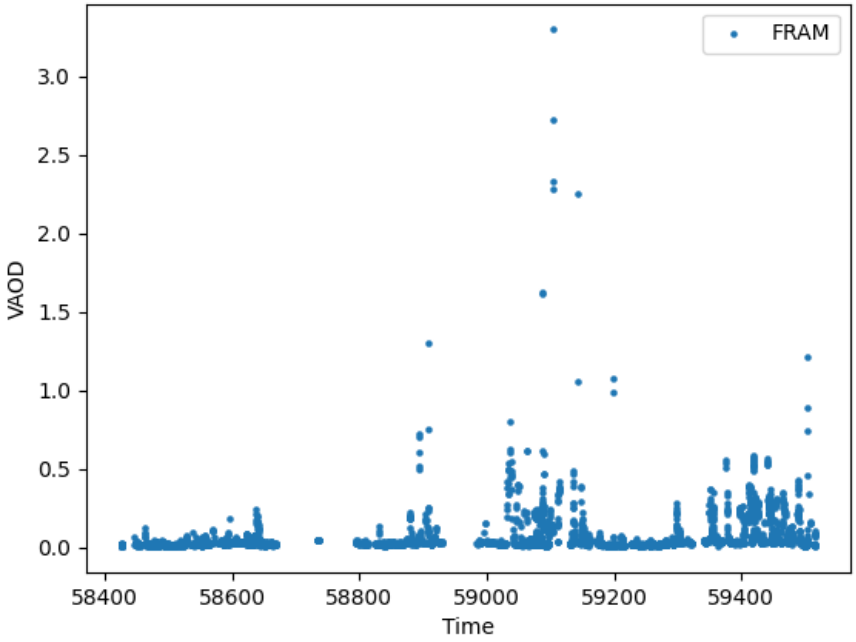

Figure 11. Variations of FRAM VAOD over time

Furthermore, the data from CTA FRAM is illustrated in *Figure 11*. The measurements were conducted in the period from 2. November, 2018, to 29. October, 2021. Similarly, through data analysis, we filtered out nonsensical data points (negative VAOD values). The graph vividly illustrates the behavior of VAOD over time. We observe peaks indicating the presence of clouds in the sky during the study period. Similar to LIDAR, FRAM also experienced measurement gaps during certain time periods, resulting in missing VAOD data points.

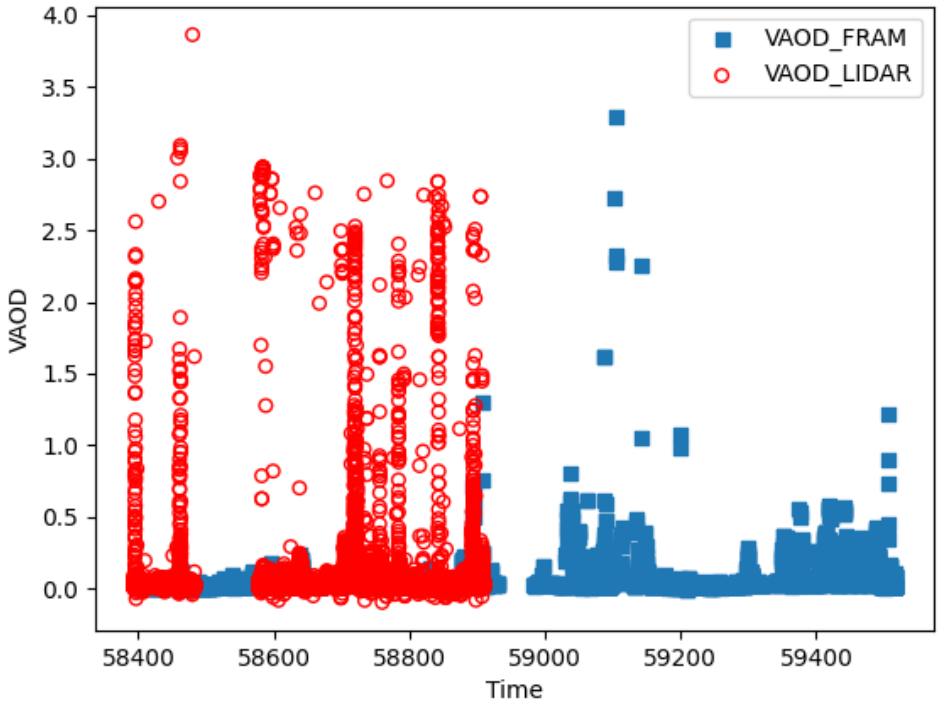

Figure 12. Data alignment for both devices over the entire time period

To facilitate a clearer observation of data relationships between FRAM and LIDAR, we have presented the dependence of VAOD over time on a single graph for both devices (*Fig. 12).* It is evident that the measurements were not conducted within the same time frame, with more data available for FRAM. To compute the correlation coefficient between LIDAR VAOD and FRAM VAOD, we need to consider data from overlapping time intervals – that is, data points that align in time. The obtained data are graphically illustrated in *Figure 12*. As LIDAR and FRAM do not capture data at precisely the same moments, we needed to approximate the data. This was achieved by using time in modified Julian days with three decimal places, providing an approximation of around 30 seconds difference. Another challenge arises from the devices not recording data at equal intervals, significantly reducing the number of data points. However, the remaining data is sufficient for calculating the correlation coefficient.

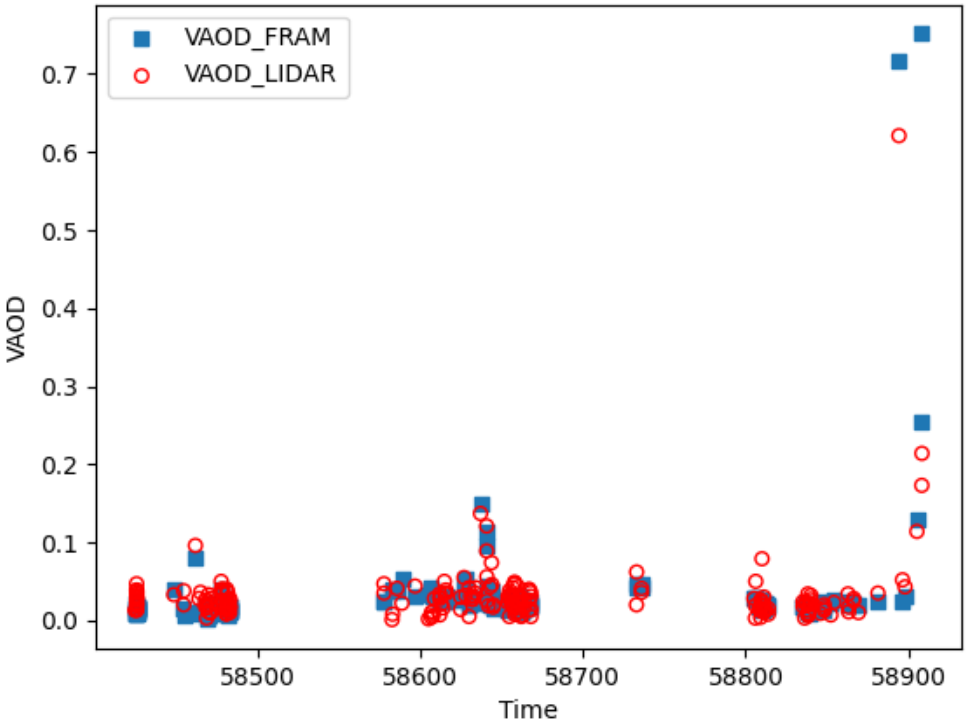

Figure 13. Data alignment for both devices over the same time period

For calculating the correlation coefficient, we employed the Python programming language. The *np.corrcoef* function from the *numpy* library serves as a versatile tool for evaluating correlation coefficients, notably encompassing the linear correlation coefficient, which is often referred to as the Pearson correlation coefficient. The obtained result is 0.8499, which is a very good outcome.

A correlation coefficient of 0.8499 indicates a relatively strong positive linear relationship between the two variables being analyzed. In general, correlation coefficients range from -1 to 1.

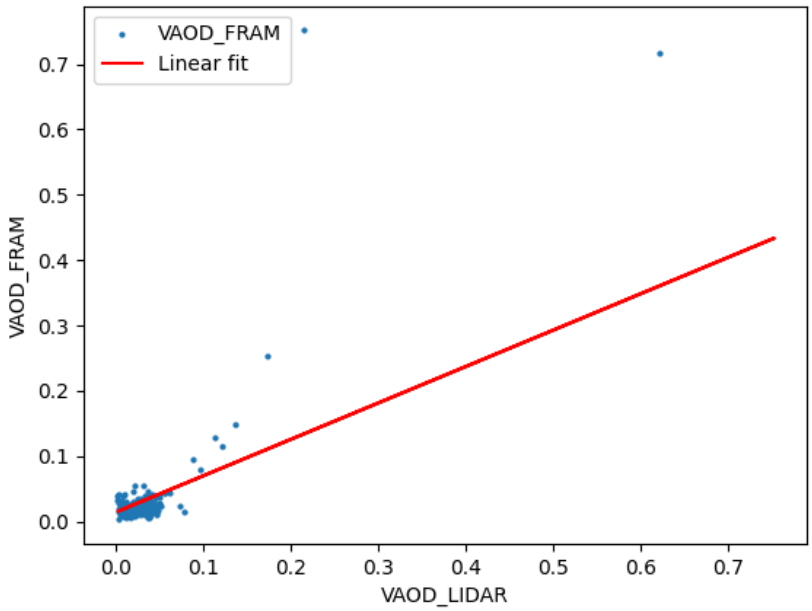

Figure 14. Dependency of LIDAR VAOD on FRAM VAOD for all data

Figure 14. illustrates the dependency of FRAM VAOD on LIDAR VAOD. A linear fit has been added to the graph to visualize the linear relationship. As the last two data points did not overlap, there was a significant data outlier. A graph excluding those data points is presented in *Figure 15.*

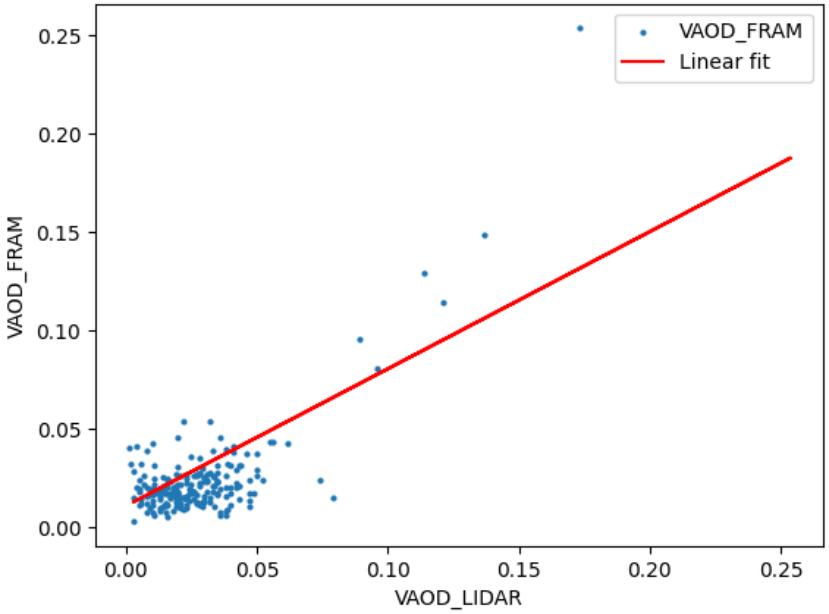

Figure 15. Dependency of LIDAR VAOD on FRAM VAOD without bad data

By calculating the linear coefficient, we obtained a value of 0.427, which does not indicate a high correlation. Therefore, it is necessary to fit other curves in order to more clearly observe the correlation for small values. At a first glance, for smaller values, the data appears to follow an exponential decay, so we attempted to fit it. By fitting, we obtained a graph shown in *Figure 16*.

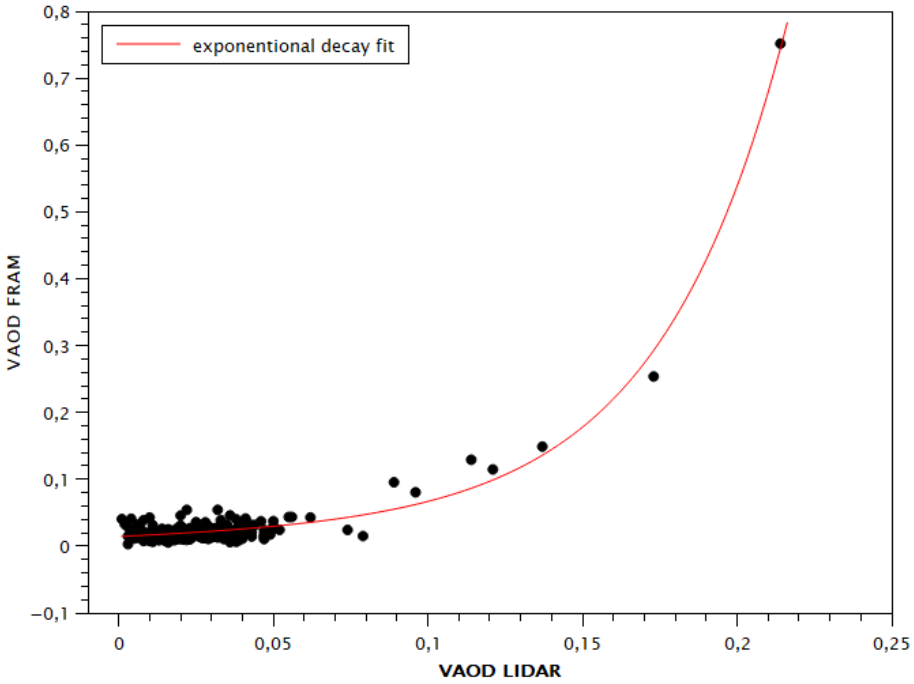

Figure 16. Fitted exponential decay

By calculating the correlation coefficient for this, we obtained a value of 0.981, which is much higher than the previous one and provides a clearer illustration of the dependence and higher correlation. More precisely, the function we obtained based on this data is equal to:

$$y = A_1 e^{\frac{-x}{t_1}} + A_2 e^{\frac{-x}{t_2}} + y_0 \tag{6}$$

We will write down the parameters and their errors below to make it clearer what their values and errors are.

$A_1 = -1.55 \cdot 10^5 \mp 1.03 \cdot 10^{12}$

$t_1 = 1.27 \cdot 10^6 \mp 8.42 \cdot 10^{12}$

$A_2 = 3.88 \cdot 10^{-3} \mp 1.41 \cdot 10^{-3}$

$t_2 = -4.11 \cdot 10^{-2} \mp 2.65 \cdot 10^{-3}$

$y = 1.55 \cdot 10^5 \mp 1.03 \cdot 10^{12}$

We also fit several other curves, such as logarithmic, polynomial functions, and others, but the best result was obtained with exponential decay.

Thus, we can notice that by considering a wide range of VAOD values, the correlation is linear. However, when considering smaller values, the correlation becomes exponential. This finding can greatly assist us in analyzing data from LIDAR and FRAM. Additionally, with more accurate measurements and determination of the fit curve equation, we can determine parameters that can aid us, for instance, if one instrument is not functioning while the other is operational. This allows for clearer and more precise measurements regardless of which instrument is in use. Since we don't have device error values, we cannot conclude whether there might be a significant impact at lower values, and by taking all values, including higher ones, this influence diminishes. After fitting only the small dataset, a linear correlation fit with a value less than 0.5 was obtained, indicating a significant lack of linearity correlation. Therefore, we consider that device errors and other factors have a significant impact on the results.

The fit *in Figure 16.* were determined using QtiPlot. Initial and final values were chosen, as well as the function to be fitted to the data. The program calculates the correlation coefficient for the selected fit and error.

Linear correlation coefficient turned out as expected but not with perfect correlation. There are numerous reasons why the coefficient isn't close to 1. One of these reasons is the time difference of around 30 seconds between measurements. Rapidly moving clouds at the time of measurement can significantly influence the values of both FRAM VAOD and LIDAR VAOD. Another potential reason is the azimuth and zenith angles at which the devices are positioned during observations. Additionally, technical issues during measurements could also contribute to these discrepancies.

4.3. Dependency of LIDAR VAOD on altitude

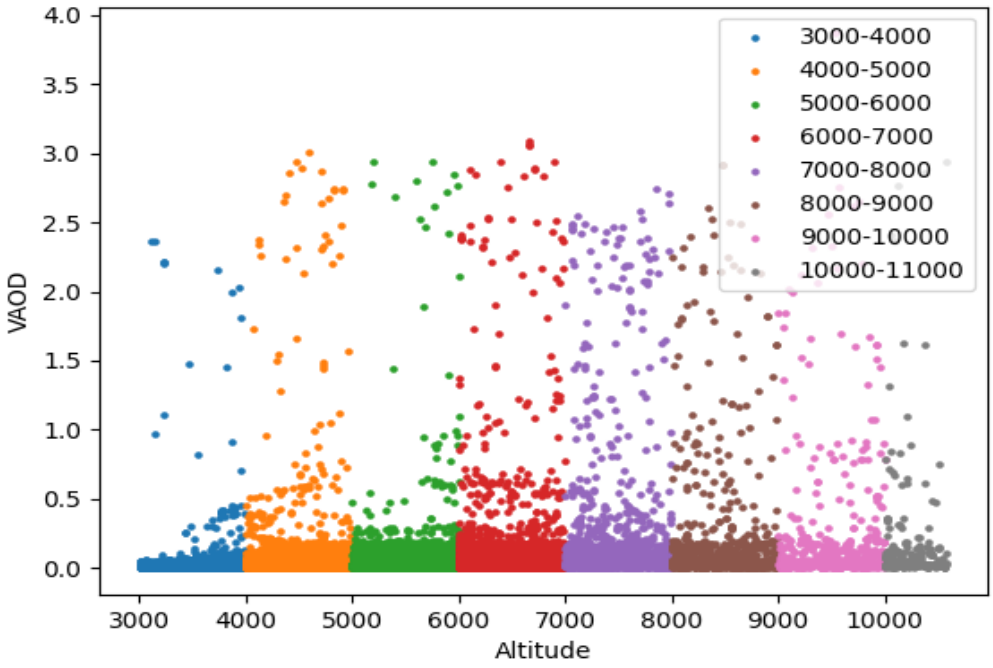

Figure 17. VAOD values depending on altitude

To observe the behavior of VAOD values concerning altitude, we have plotted all the acquired data from MAGIC LIDAR (*Fig. 17*). To enhance clarity, we have assigned colours to specific altitude ranges. At a glance, it's evident that for altitudes between 3000 to 4000 meters above the observatory, VAOD exhibits low values, with only a few data points exceeding 1. The highest VAOD values are observed at altitudes between 6000 to 9000 meters, as anticipated, given that clouds at these altitudes above the observatory significantly influence VAOD values. To depict the dependence more effectively, we have calculated the average VAOD values for each altitude interval. The resulting values are shown in Table 1.

Table 1. Average VAOD values for each altitude interval

Height interval	VAOD
3000-4000 m	0.0298
4000-5000 m	0.0427
5000-6000 m	0.0502
6000-7000 m	0.0941
7000-8000 m	0.1596
8000-9000 m	0.1623
9000-10000 m	0.1795
10000-11000 m	0.1699

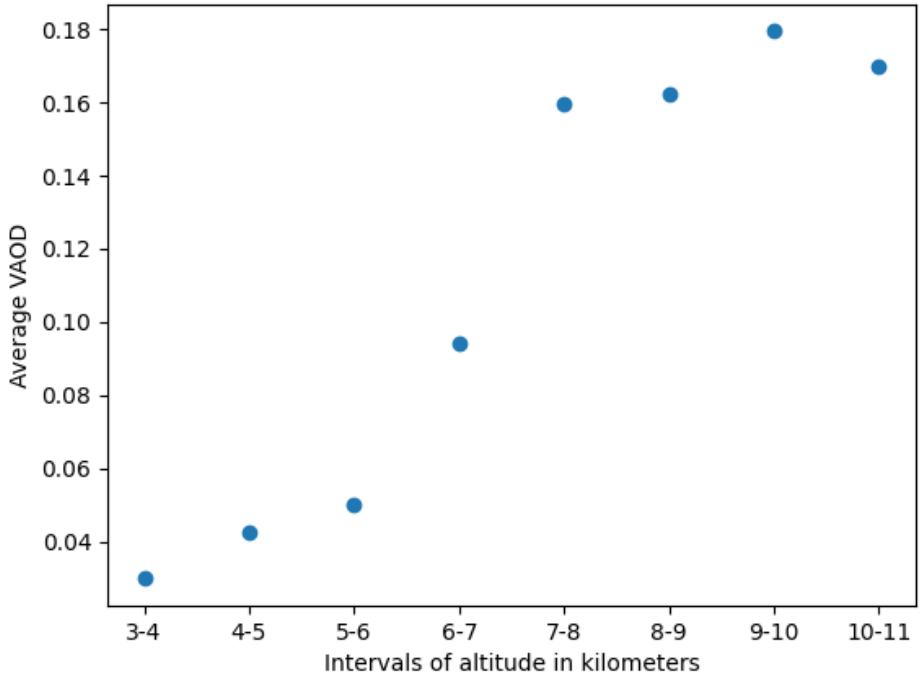

Figure 17. Average VAOD values for altitude intervals

Furthermore, the average values have been plotted on the graph shown in *Figure 19*. It's evident that for lower altitudes above the observatory, the average values are smaller. A rise in VAOD values can be observed up to an altitude of 10000 meters, beyond which they start to decrease again. The graph clearly depicts that the highest values are found at an altitude range between 9000 and 10000 meters, which aligns with the theoretical understanding due to the presence of clouds at those altitudes influencing VAOD values.

5. CONCLUSION

In this study we were focusing on the Vertical Aerosol Optical Depth (VAOD) as a key parameter to understand aerosol behaviour in the atmosphere.

The data presented in the previous text provides valuable insights into the behaviour of VAOD (Vertical Aerosol Optical Depth) measured by MAGIC LIDAR and CTA FRAM over time. The analysis revealed several important findings and challenges.

Firstly, irregularities in the data, such as negative VAOD values and sporadic high VAOD values, were observed due to technical issues and imperfections in the devices' operation. These issues led to the exclusion of certain data points and missing measurements, impacting the overall dataset's completeness.

The correlation coefficient of 0.8499 between LIDAR VAOD and FRAM VAOD indicates a relatively strong positive linear relationship between the two variables. However, the coefficient is not close to 1, suggesting that other factors, such as the time difference of around 30 seconds between measurements is rapidly moving clouds and the devices azimuth and zenith angles, contribute to the differences in the data.

It's noteworthy to mention that while linear correlation is suitable for broader intervals, for lower VAOD values, exponential decay function show better efficacy, with correlation coefficient 0.98.

By examining the VAOD values concerning altitude, it was evident that lower altitudes above the observatory exhibit smaller average VAOD values, while a rise in VAOD values was observed up to an altitude of 10000 meters. The altitude analysis demonstrated that VAOD values were higher particularly between 6000 and 10000 meters, corresponding to the presence of clouds.

The highest VAOD values were found between 9000 and 10000 meters, which aligns with the expected influence of clouds at those altitudes on VAOD values.

The findings from this analysis offer valuable insights into the dynamic nature of VAOD and its association with altitude and cloud presence over time. However, it is essential to acknowledge the technical challenges and data limitations encountered during the measurements. These challenges underscore the significance of continuous improvements in device operation and measurement techniques to ensure the accuracy and comprehensiveness of future data.

In forthcoming studies, it is absolutely crucial to tackle these technical challenges head-on and ensure that measurements are carried out consistently within well-defined time frames. By doing so, we can undoubtedly achieve a more reliable correlation analysis and gain a deeper comprehension of how aerosols behave in the atmosphere. This newfound knowledge bears immense significance for diverse atmospheric and climate-related investigations, considering the pivotal role aerosols play in influencing Earth's radiative balance and overall climate system.

LITERATURE

[1] B. Bechtel, The climate of the Canary Islands by annual cycle parameters, The International Archives of the Photogrammetry, Remote Sensing and Spatial Information Sciences, Volume XLI-B8, 2016 XXIII ISPRS Congress, Prague, Czech Republic, 2016

[2] S. BenZvi, M. Bohacova, B. Connolly, J. Grygar, M. Hrabovsky, T. Karova, D. Mandat, P. Necesal, D. Nosek, L. Nozka, M. Palatka, M. Pech, M. Prouza, J. Ridky, P. Schovanek, R. Smida, P. Travnicek, P. Vitale, S. Westerhoff, New method for atmospheric calibration at the Pierre Auger Observatory using FRAM, a robotic astronomical telescope, Argentina, arXiv:0706.1710**,** 2007

[3] K. Bernlohr, Shower detection, URL: https://www.mpi-hd.mpg.de/hfm/CosmicRay/ShowerDetection.html (9.9.2023.)

[4] R. A. Dastrup, Dynamic Earth: Introduction to Physical Geography, URL: https://courses.lumenlearning.com/suny-geophysical/chapter/layers-of-the-atmosphere/ (7.8.2023.)

[5] J. Holder, Atmospheric Cherenkov Gamma-ray Telescopes, World Scientific Volume, arXiv:1510.05675, 2015.

[6] J. Ebr,1 P. Janecek, M. Prouza, P. Kubanek, M. Jelınek, M. Masek, I. Ebrova´, J. Cerny, FRAM: SHOWERS, COMETS, GRBS AND POPULAR SCIENCE, Revista Mexicana de Astronomía y Astrofísica, vol. 45, 2014, pp. 114-117 Instituto de Astronomía Distrito Federal, México

[7] J. Ebr, J. Juryšek, M. Prouza, J.Blažek, P.Travniček, D. Mandat, M.Pech, New developments in aerosol measurements using stellar photometry, 1 Prague , EPJ Web of Conferences 197, 2019

[8] J. Ebr , D. Mandáta , M. Pech , L. Chytka , J. Juryšek , M. Prouza , P. Janecek, P. Trávnícek J. Blažek, T. Bulik , M. Cieslar , M. Suchenek , V. Rizie , E. Pietropaolo , M. Iarlori , C. Aramo, L. Valore , F. Di Pierro , P. Vallania , D. Depaoli , M. Will, M. Gaug, L. Font , M. Mašeka , J. Eliášek, M. Jelíneki, S. Karpova, Characterization of atmospheric properties at the future sites of the Cherenkov Telescope Array, arXiv:1909.08088, 2019

[9] R. G. Fleagle, J. A. Businger, An Introduction to Atmospheric Physics, Academic press, Washington, 2nd edition, 1980.

[10] C. Fruck, M. Gaug, A. Hahn, V. Acciari, J. Besenrieder, D. Dominis Prester, D. Dorner, D. Fink, L. Font, S. Mičanović, R. Mirzoyan, D. Muller, L. Pavletić, F. Schmuckermaier, M.Will, Characterizing the aerosol atmosphere above the Observatorio del Roque de los Muchachos by analyzing seven years of data taken with an GaAsP HPD-readout, absolutely calibrated elastic LIDAR, arXiv:2202.09561**,** MNRAS 000, 1–36, 2022

[11] C. Fruck, M.Gaug, R. Zanin, D. Dorner, D. Garrido, R. Mirzoyan, L. Font, A novel LIDAR-based Atmospheric Calibration Method for Improving the Data Analysis of MAGIC, arXiv:1403.3591**,** 2014

[12] P. Janecek , J. Ebr, J. Blažek, M. Prouza , M. Mašek, J. Eliášek, FRAM for the Cherenkov Telescope Array: an update, Institute of Physics of the Czech Academy of Sciences, Prague, EPJ Web Conferences 144, 2017

[13] P. Janecek, J. Ebr, J. Juryšek, M. Prouza, J. Blažek, P. Trávnícek, D. Mandát, M. Pech, S. Karpov, R. Cunniffe, M. Mašek, M. Jelínek, I. Ebrová, FRAM telescopes and their measurements of aerosol content at the Pierre Auger Observatory and at future sites of the Cherenkov Telescope Array, EPJ Web of Conferences 197, 02008, 2019

[14] D. Mandat, M. Pech, M. Hrabovsky, P. Schovanek, M. Palatka, M. Prouza, P. Travnicek, P. Janecer, J. Ebr, M. Doro, M. Gaug, All Sky Camera for the CTA Atmospheric Calibration work package EPJ Web Conferences 89, 03007, 2015

[15] F. Schmuckermaier, M. Gaug, C. Fruck, A. Moralejo, A. Hahn, D. Dominis Prester, D. Dorner, L. Font, S. Mićanović, R. Mirzoyan, D. Paneque, L. Pavletić, J. Sitarek, M. Will, Correcting Imaging Atmospheric Cherenkov Telescope data with atmospheric profiles obtained with an elastic light detecting and ranging system, arXiv:2302.12072**,** 2023

[16] The Pierre Auger Collaboration et al., The FRAM robotic telescope for atmospheric monitoring at the Pierre Auger Observatory, Mendoza, Argentina, arXiv:2101.11602 **,** 2021

[17] F. Schmuckermaier, M. Gaug, C. Fruck, A. Moralejo, A. Hahn, D. Dominis Prester, D. Dorner, L. Font, S. Mićanović, R. Mirzoyan, D. Paneque, L. Pavletić, J. Sitarek, M. Will, Correcting Imaging Atmospheric Cherenkov Telescope data with atmospheric profiles obtained with an elastic light detecting and ranging system, arXiv:2302.12072**,** 2023

[18] J. M. Wallace P.V. Hobbs, Atmospheric Science, Academic press, Washington, 2nd edition, 2006

LIST OF IMAGES

LIST OF TABLES